Circular photon drag effect in bulk tellurium

V. A. Shalygin,[1,2] M. D. Moldavskaya,[1] S. N. Danilov,[2] I. I. Farbshtein,[3] and L. E. Golub[3]
[1]*Department of Physics of Semiconductors and Nanoelectronics, Peter the Great St. Petersburg Polytechnic University, St. Petersburg 195251, Russia*
[2]*Terahertz Center, University of Regensburg, Regensburg 93040, Germany*
[3]*Ioffe Institute, St. Petersburg 194021, Russia*
(Received 14 October 2015; revised manuscript received 4 January 2016; published 21 January 2016)

The circular photon drag effect is observed in a bulk semiconductor. The photocurrent caused by a transfer of both translational and angular momenta of light to charge carriers is detected in tellurium in the midinfrared frequency range. Dependencies of the photocurrent on the light polarization and on the incidence angle agree with the symmetry analysis of the circular photon drag effect. Microscopic models of the effect are developed for both intra- and intersubband optical absorption in the valence band of tellurium. The shift contribution to the circular photon drag current is calculated. An observed decrease of the circular photon drag current with the increase of the photon energy is explained by the theory for intersubband optical transitions. Theoretical estimates of the circular photon drag current agree with the experimental data.

DOI: 10.1103/PhysRevB.93.045207

I. INTRODUCTION

Circularly polarized light has an angular momentum which can be transferred to charge carriers. The transfer of angular momentum from light to charge particles is studied in various fields of condensed-matter physics, in particular in semiconductors and metals [1,2]. Interaction of circularly polarized light with matter results in spin orientation of free carriers [3], in magnetization control by light in magnetic materials [4], and in generation of charge and spin currents in semiconductor and ferromagnetic structures [5–7] and graphene [8–10].

The presence or absence of the light angular momentum depends on its polarization state. However, a light wave always carries a translational momentum. First demonstrated by Lebedev in his classical experiment [11], light translational momentum has been detected in semiconductors by an electrical current. The current is generated by the transfer of the translational momentum from light to charge carriers (see, e.g., Refs. [12,13] and references therein). The photocurrent generation due to this mechanism is known as the photon drag effect. It is investigated as a fundamental phenomenon in various media, e.g., in semiconductors [13] and dielectrics [14], and has practical application in work of photodetectors [13,15–17]. Now the photon drag effect is intensively being studied in graphene for material characterization [8] and generation of terahertz radiation [18–20], in carbon nanotubes [21], and in thin-metal films, where the photon drag current is enhanced in the vicinity of surface plasmon resonance [22].

An additional control over the photon drag current can be made at simultaneous transfer of both angular and translational momenta from light to charge carriers. There is a part of the photon drag current which is sensitive to the light helicity and reverses its direction on switching from right- to left-circular polarization of light. Generation of the helicity-dependent photon drag current is known as a circular photon drag effect (CPDE). In contrast to the intensively studied photon drag currents insensitive to the circular polarization, the history of CPDE is rather short. While CPDE was discovered theoretically in the 1980s in Refs. [23,24] and some theoretical research was done in the next decade [25], experimentally, it was demonstrated only in 2007 by studying quantum wells [26,27]. Further experiments also deal exclusively with two-dimensional systems as photonic crystal slabs [28], graphene [29–31], metamaterials [32], and quantum-well structures [33]. Most recently, CPDE became the focus of investigations of two-dimensional surface states in topological insulators [34,35] with the aim to realize optical control of spin currents and to characterize high-frequency electron transport in these novel materials. However, CPDE has not been observed so far in bulk systems. The reason is that CPDE is forbidden by symmetry in cubic crystals like III–V semiconductors, or it is masked by other effects in those media where it is allowed. In this work, we address the fundamental question of whether the transfer of both angular and translational momenta is possible in three-dimensional structures.

We report on the observation of CPDE in a bulk semiconductor demonstrating that the photon drag current sensitive to the light helicity is indeed possible in three-dimensional systems. For this purpose we choose tellurium, which demonstrates a few related phenomena, namely, electric-current-induced optical activity, the linear photon drag effect, and linear and circular photogalvanic effects [13,36]. In contrast to the two-dimensional systems [26,27], for tellurium we can choose a particular geometry where CPDE is not hidden by any other effect. We show that the values of the CPDE current are two orders of magnitude higher than in quantum well structures.

This paper is organized as follows. In Sec. II, the phenomenological analysis of photocurrents in tellurium is performed. In Sec. III we present results of experimental observation of the CPDE current. In Sec. IV, the microscopic theory of CPDE is developed. Section V discusses the obtained results, and Sec. VI concludes the paper.

II. DETERMINATION OF EXPERIMENTAL GEOMETRY

In order to choose a proper geometry for observation of the CPDE current we perform the symmetry analysis of helicity-dependent photocurrents in tellurium. The point symmetry group of tellurium is D_3. In the plane perpendicular

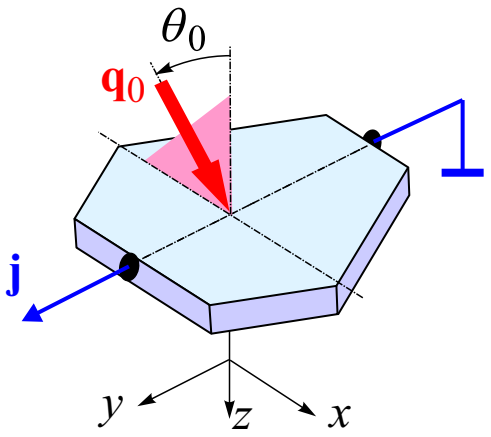

FIG. 1. The experimental geometry.

to the optical axis z, there are three rotation axes C_2', which form an angle of 120° with each other. We denote one of them as x and also denote a perpendicular axis in the same plane as y (see Fig. 1). We consider a radiation incident in the plane (xz). Performing a symmetry analysis, we obtain the photocurrent which reverses its direction under switching from right-hand- to left-hand-polarized radiation. The density of this photocurrent $\boldsymbol{j}^{\rm circ}$ proportional to the circular polarization degree of light $P_{\rm circ}$ is given by

$$j_z^{\rm circ} = \gamma P_{\rm circ} \frac{q_z}{q} E^2, \tag{1}$$

$$j_x^{\rm circ} = \tilde{\gamma} P_{\rm circ} \frac{q_x}{q} E^2 + \tilde{T} P_{\rm circ} \frac{q_x^2}{q} E^2, \tag{2}$$

$$j_y^{\rm circ} = T P_{\rm circ} \frac{q_x q_z}{q} E^2. \tag{3}$$

Here $\boldsymbol{q}$ and $\boldsymbol{E}$ are the radiation wave vector and electric field, respectively, and $E = |\boldsymbol{E}|$. The constants γ and $\tilde{\gamma}$ describe the circular photogalvanic effect caused solely by transfer of an angular momentum of photons to free carriers but not accompanied by a linear momentum transfer. The longitudinal CPDE current described by the constant $\tilde{T}$ is present due to a trigonal symmetry of tellurium. The transverse CPDE described by the constant T is caused by a nonequivalence of the z direction and the directions in the perpendicular plane (xy), i.e., due to uniaxiality of tellurium. This CPDE current is odd in the incidence angle θ_0.

Equations (1)–(3) demonstrate that the current $j_y^{\rm circ}$ is caused solely by the CPDE, in contrast to two other photocurrent components. Therefore in the experimental part we focus on the photocurrent transverse to the incidence plane (xz).

III. OBSERVATION OF CPDE

Experimental investigations were performed on a p-Te single crystal, which is characterized at room temperature by the concentration $p = 7 \times 10^{16}$ cm^{-3} and the hole mobility $\mu = 700$ cm^2/(V s). The tellurium single crystal was grown by the Czochralski method in a hydrogen atmosphere. The samples had the form of a hexagonal prism, in which the lateral surface was a natural facet of the crystal, and the end faces were subjected to optical polishing. It was found that the crystal under investigation exhibits a natural optical activity and is levorotatory. The thickness of the sample in the direction of the crystal optical axis z was $L = 0.8$ mm. To measure the photocurrent J_y in the direction perpendicular to the incidence plane, two contacts were located at the lateral surface of the sample. The contacts were prepared from an alloy of tin, bismuth, and antimony with a low melting temperature (Sn:Bi:Sb = 50:47:3). A few samples fabricated from the same single crystal were studied and demonstrated similar results.

We applied midinfrared radiation of a tunable Q-switched as well as pulsed transversely excited atmosphere (TEA) CO_2 lasers with an operating spectral range from 9.2 to 10.8 μm, corresponding to photon energies ranging from 114 to 135 meV [37,38]. The laser pulses had a peak power P of about 500 W (for TEA laser after attenuation), the pulse duration was 100–250 ns, and the repetition frequency was up to 160 Hz for the Q-switch laser and near 1 Hz for the TEA laser. The radiation power was controlled by a room-temperature photon drag [39,40] and mercury cadmium telluride detectors. The radiation was focused on a spot of 0.5 mm diameter, which is much smaller than the sample sizes in the x and y directions (8 and 7 mm, respectively). The spatial beam distribution has an almost Gaussian profile, measured by a pyroelectric camera [41,42]. The photocurrent was measured by means of a storage oscilloscope.

The upper end face of the sample was illuminated by a laser beam under incidence angle θ_0, which is defined as the angle between the wave vector of the incident radiation $\boldsymbol{q}_0$ and the z axis. The angle θ_0 shown in Fig. 1 is positive. The incidence plane (xz) contains the crystallographic axis x, which is the twofold rotation axis C_2'. The laser radiation was linearly polarized. By applying a Fresnel $\lambda/4$ rhomb we modified the radiation polarization from linear to elliptical. The circular polarization of the light at the Fresnel rhomb output $P_{\rm circ}^0$ was varied from -1 (left-handed circular polarization σ_-) to $+1$ (right-handed σ_+) according to $P_{\rm circ}^0 = \sin 2\varphi$, where φ is the azimuth of the Fresnel rhomb.

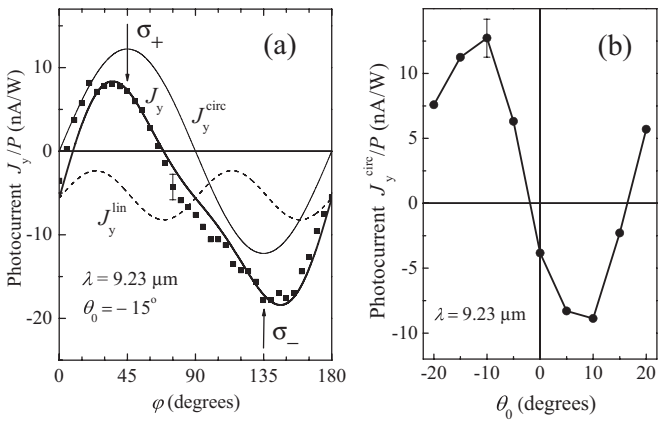

FIG. 2. (a) The transverse photocurrent dependence on the Fresnel rhomb rotation angle. $J_y^{\rm circ} \propto \sin 2\varphi$ and $J_y^{\rm lin}$ represent the circular and linear photocurrents, respectively. (b) The dependence of the circular photocurrent on the incidence angle at the Fresnel rhomb azimuth $\varphi = 45°$.

Figure 2(a) shows the typical dependence of the transverse photocurrent J_y normalized to the laser power P on the Fresnel rhomb azimuth under oblique incidence of the laser beam (at $\theta_0 = -15^\circ$). The photocurrent at each azimuthal angle φ depends linearly on the laser power P. The experimental data are well described by the following phenomenological expression:

$$J_y = C \sin 2\varphi + L_1 \sin 4\varphi + L_2, \tag{4}$$

where the first term is proportional to $P^0_{\rm circ}$ and corresponds to the "circular" photocurrent $J_y^{\rm circ}$ which we are interested in. Two other terms represent the "linear" photocurrent $J_y^{\rm lin}$ which appears under elliptically polarized excitation. The linear photocurrent is insensitive to the radiation helicity. The photocurrent has a substantial part dependent on the light helicity. Figure 2(a) shows that the photocurrent has opposite directions at excitation by right-handed (σ_+) and left-handed (σ_-) polarized light.

In order to extract the current sensitive to the light helicity, $J_y^{\rm circ} = C \sin 2\varphi$, we perform analysis of the φ dependencies of the transverse photocurrent J_y at various incidence angles. This allows us to reveal the dependence of the circular photocurrent amplitude C on θ_0. It is presented in Fig. 2(b). One can see that the circular photocurrent is mainly an odd function of θ_0 with an admixture of a small even contribution.

According to the phenomenological arguments in Sec. II, the CPDE current is an odd function of the incidence angle. Therefore we continued our analysis studying the odd in θ_0 part of $J_y^{\rm circ}$. It is defined as follows:

$$J_{\rm odd}(\theta_0) = \frac{C(\theta_0) - C(-\theta_0)}{2}.$$

The dependence of $J_{\rm odd}$ on the incidence angle is plotted in Fig. 3. We note that the helicity-dependent current exceeds by two orders of magnitude the current detected in quantum-well structures [26,27]. We performed the same measurements and analysis at three other photon energies. The obtained dependence of $|J_{\rm odd}|$ on the photon energy is shown in the inset in Fig. 3.

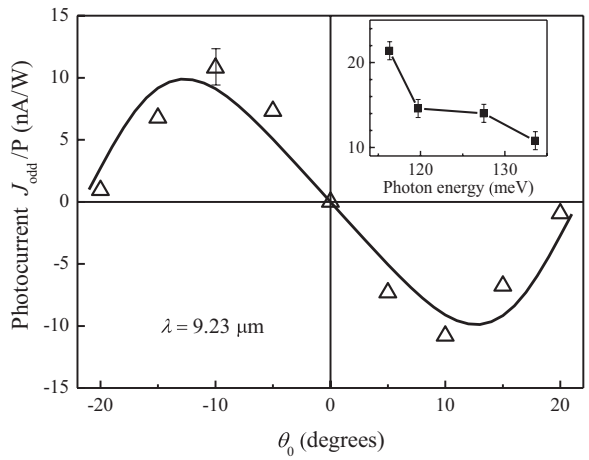

FIG. 3. Symbols: the circular photocurrent odd in the incidence angle θ_0. The line is a fit by $\bar{j}(\theta_0)$ given by Eq. (10). The inset shows the dependence of $|J_{\rm odd}|/P$ on the photon energy at $\theta_0 = 10^\circ$.

In order to verify that the odd in θ_0 photocurent $J_{\rm odd}$ is caused by the CPDE, it is necessary to derive the dependence of CPDE on the incidence angle and to compare it with the experimental data. However, it is not a trivial problem because tellurium is a birefringent crystal. It is characterized by two substantially different components of the dielectric susceptibility tensor, $\varepsilon_\perp = 23$ and $\varepsilon_\parallel = 36$ for light polarized perpendicular and parallel to the optical axis z, respectively. At an oblique incidence (see Fig. 1), the light beam splits inside the medium into ordinary (o) and extraordinary (e) beams. The z components of the vectors $c\boldsymbol{q}/\omega$ for these beams are respectively given by

$$n_o = \sqrt{\varepsilon_\perp - \sin^2\theta_0}, \quad n_e = \sqrt{\varepsilon_\perp - \frac{\varepsilon_\perp}{\varepsilon_\parallel}\sin^2\theta_0}. \tag{5}$$

Therefore the dependence of CPDE current on θ_0 is a complicated function, in contrast to the case of quantum-well structures, and deriving this dependence is an independent problem.

The transverse CPDE current equation (3) can be equivalently presented as

$$j_y^{\rm circ} = T q_x i (E_x E_y^* - E_y E_x^*). \tag{6}$$

Since the ordinary and extraordinary beams propagate with different velocities, the CPDE current [equation (6)] oscillates in space along the propagation direction like other helicity-dependent photocurrents in birefringent crystals [43]. The period of these space oscillations is given by

$$d(\theta_0) = \frac{\lambda}{n_o - n_e}, \tag{7}$$

where $\lambda = 2\pi c/\omega$ is the wavelength in vacuum. The current density dependence on the coordinate z inside the sample is the following:

$$j_y^{\rm circ}(z) = T q_x \cos\left[\frac{2\pi z}{d(\theta_0)}\right] P^0_{\rm circ} \mathcal{T}_{ps}(\theta_0) E_0^2, \tag{8}$$

where E_0 is the radiation amplitude in vacuum and the transmission coefficient is given by (see the Appendix)

$$\mathcal{T}_{ps}(\theta_0) = \frac{4 n_e \cos^2\theta_0}{(\cos\theta_0 + n_o)(\varepsilon_\perp \cos\theta_0 + n_e)}. \tag{9}$$

As a result, the CPDE current density in a sample of thickness L depends on θ_0 as follows:

$$\frac{1}{L}\int_0^L dz\, j_y^{\rm circ}(z) \equiv \bar{j}(\theta_0) = T\frac{\omega}{c} P^0_{\rm circ} E_0^2 \mathcal{T}_{ps}(\theta_0) \sin\theta_0 \frac{\sin[2\pi L/d(\theta_0)]}{2\pi L/d(\theta_0)}. \tag{10}$$

The absolute value of the experimentally detected photocurrent $|J_{\rm odd}(\theta_0)|$ is proportional to the average current density given by Eq. (10). The fit of the experimental data by the function $\bar{j}(\theta_0)$ is shown by a solid line in Fig. 3. One can see good agreement between the theory and the experimental data. Note the importance of birefringence in our experiment: although the angular dependence $\mathcal{T}_{ps}(\theta_0)\sin\theta_0$ is almost linear in the studied range $|\theta_0| < 20^\circ$, the function $\bar{j}(\theta_0)$

has a maximum at $\theta_0 \approx 13^\circ$ and tends to zero at $\theta_0 \approx 20^\circ$, in agreement with experimental data. This is a clear signature of the birefringence making the period $d(\theta_0)$ comparable to the sample thickness at moderate incidence angles.

The above analysis of the photocurrent dependencies on the laser power, polarization state, and incidence angle confirms the observation of CPDE.

IV. MICROSCOPIC THEORY

Now we develop a microscopic theory of CPDE in tellurium. We derive the photon energy dependence of the CPDE current and compare it with the experimental data.

The effective Hamiltonian of holes in the tellurium valence band has the form [44]

$$H(\boldsymbol{k}) = Ak_z^2 + Bk_\perp^2 + \beta\sigma_z k_z + \Delta\sigma_x, \tag{11}$$

where $\boldsymbol{k}$ is a hole wave vector and σ_z, σ_x are the Pauli matrices. The valence band is split at $k > 0$ on two subbands with the dispersions

$$E_{1,2}(\boldsymbol{k}) = Ak_z^2 + Bk_\perp^2 \mp \sqrt{\Delta^2 + \beta^2 k_z^2}, \tag{12}$$

which are plotted in Fig. 4.

We calculate the CPDE constant T in Eqs. (3) and (6) for both intrasubband and intersubband absorption in the tellurium valence band.

A. Drude-like absorption

At low frequencies $\hbar\omega \ll \Theta$, where Θ is the temperature in energy units, light absorption is caused by intraband transitions. The CPDE current at Drude-like absorption is found by solving the Boltzmann kinetic equation. In order to get the CPDE photocurrent, we take into account both the coordinate dependence of the distribution function and the Lorentz force caused by the magnetic field $\boldsymbol{B}$ of the light wave. In the relaxation-time approximation, the Boltzmann equation for the distribution function f dependent on the hole wave vector $\boldsymbol{k}$, coordinate $\boldsymbol{r}$, and time t has the form

$$\frac{\partial f}{\partial t} + \boldsymbol{v_k}\cdot\frac{\partial f}{\partial \boldsymbol{r}} + \frac{e}{\hbar}\boldsymbol{E}\cdot\frac{\partial f}{\partial \boldsymbol{k}} + \frac{e}{\hbar c}(\boldsymbol{v_k}\times\boldsymbol{B})\cdot\frac{\partial f}{\partial \boldsymbol{k}} = -\frac{f-\bar{f}}{\tau}. \tag{13}$$

Here the overbar denotes averaging over directions of $\boldsymbol{k}$, τ is the momentum relaxation time, and $\boldsymbol{v_k} = \hbar^{-1}\partial\varepsilon_{\boldsymbol{k}}/\partial\boldsymbol{k}$ is the hole velocity, with $\varepsilon_{\boldsymbol{k}} \equiv E_1(\boldsymbol{k})$ being the hole energy dispersion in the ground valence subband. The photocurrent density is given by

$$\boldsymbol{j} = 2e\sum_{\boldsymbol{k}} \boldsymbol{v_k}\langle f(\boldsymbol{k},\boldsymbol{r},t)\rangle, \tag{14}$$

where the factor 2 accounts for two tellurium valleys and angular brackets indicate averaging over both the space coordinate and time.

Solving the Boltzmann equation by iterations in the second order in $\boldsymbol{E}$ and in the first order in the space gradient at $B = 0$, we find the first part of the CPDE current. Taking into account both $\boldsymbol{E}$ and $\boldsymbol{B}$ in the first orders but ignoring the coordinate dependence, we get the second part [8,29]. As a result, we obtain the CPDE current density in the form

$$j_y^{\text{circ,Drude}} = q_x i(E_x E_y^* - E_y E_x^*) \times 2e^3\sum_{\boldsymbol{k}}\frac{d\tau}{d\varepsilon_{\boldsymbol{k}}}\frac{\tau^2(-df_0/d\varepsilon_{\boldsymbol{k}})}{[1+(\omega\tau)^2]^2}v_\perp^2\left(\frac{v_\perp^2}{2} - \frac{\varepsilon_\perp}{\varepsilon_\parallel}v_z^2\right). \tag{15}$$

Here $f_0(\varepsilon_{\boldsymbol{k}})$ is the Boltzmann distribution function, and $v_\perp^2 = v_x^2 + v_y^2$. Deriving this expression, we have taken into account the relation $\mathrm{div}\boldsymbol{D} = 0$, which yields

$$\varepsilon_\parallel q_z E_z + \varepsilon_\perp \boldsymbol{q}_\perp\cdot\boldsymbol{E}_\perp = 0. \tag{16}$$

B. Intersubband transitions

At photon energy larger than the intersubband gap, $\hbar\omega > 2\Delta$, light absorption is caused by direct optical transitions. The CPDE current can be calculated in this case by quantum-mechanical methods. The analysis shows that the CPDE current is a sum of two terms. The first, the *ballistic* contribution, arises from accounting for an additional scattering process side by side with the optical transition [24]. The second contribution, called the *shift* photocurrent, is caused by shifts of carriers in real space occurring at photon absorption [12]. We estimate the value of the CPDE current calculating the shift contribution.

The shift photocurrent density at direct optical transitions is given by

$$\boldsymbol{j}^{\text{inter}} = -2e\sum_{\boldsymbol{k}}\frac{2\pi}{\hbar}\delta[E_2(\boldsymbol{k}+\boldsymbol{q}) - E_1(\boldsymbol{k}) - \hbar\omega] \times\{f_0[E_1(\boldsymbol{k})] - f_0[E_2(\boldsymbol{k}+\boldsymbol{q})]\}\,\mathrm{Im}(V_{21}^*\nabla_{\boldsymbol{k}}V_{21}), \tag{17}$$

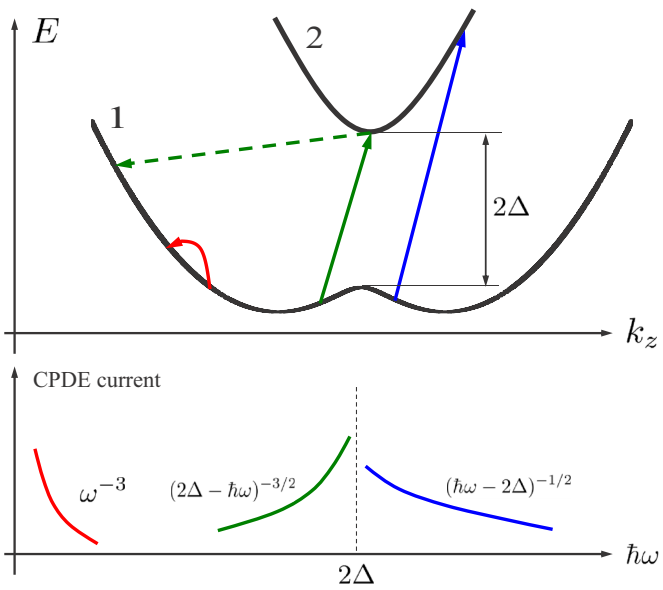

FIG. 4. Top: The valence-band diagram of tellurium in the hole representation. A red arrow denotes optical intrasubband transition at low frequency, green arrows indicate a transition of the same type with an intermediate state in the excited subband accompanied by intersubband scattering (dashed arrow), and a blue arrow shows the direct intersubband optical transition. Bottom: Frequency dependencies of the CPDE current absolute value in three frequency ranges corresponding to the transitions indicated in the top panel.

where V_{21} is a matrix element of the operator of direct optical transitions accounting for the photon wave vector $\boldsymbol{q}$. The wave-function envelopes are eigenvectors of the Hamiltonian (11): $\Psi_1 = (C_1, C_2)$, $\Psi_2 = (C_2, -C_1)$, where $C_{1,2} = \sqrt{(1 \pm \eta)/2}$, $\eta = \beta k_z / \sqrt{\Delta^2 + \beta^2 k_z^2}$ [44]. The direct optical transitions at $q = 0$ are allowed only in the polarization $\boldsymbol{E} \parallel z$. However, by accounting for the photon momentum, the polarization $\boldsymbol{E}_\perp \perp z$ also interacts with the carriers:

$$V_{21} = \frac{ie\beta\Delta}{\hbar\omega}\left(\frac{E_z}{\sqrt{\Delta^2 + \beta^2 k_z^2}} - Bq_z \frac{\boldsymbol{E}_\perp \cdot \boldsymbol{k}_\perp}{\Delta^2 + \beta^2 k_z^2}\right). \quad (18)$$

It follows from this equation that the coordinate shifts of holes in the y direction proportional to the light helicity are present at $q \neq 0$ [45]:

$$\Delta y \sim -\frac{\mathrm{Im}(V_{21}^* \partial V_{21}/\partial k_y)}{|V_{21}|^2} \sim P_{\mathrm{circ}} \frac{Bq}{\sqrt{\Delta^2 + \beta^2 k_z^2}}. \quad (19)$$

A calculation using Eq. (17) accounting for relation (16) leads to the CPDE current in the form

$$j_y^{\mathrm{circ,inter}} = -q_x i(E_x E_y^* - E_y E_x^*) \frac{8\pi p e^3 B|\beta|\Delta^2\sqrt{A}\varepsilon_\perp}{J\hbar^5\omega^4\sqrt{\Theta}\varepsilon_\parallel} \times (1 - e^{-\hbar\omega/\Theta}) \times \frac{\exp\left\{-\frac{A}{4\beta^2\Theta}[(\hbar\omega)^2 - (2\Delta)^2] + \frac{\hbar\omega - 2\Delta}{2\Theta}\right\}}{\sqrt{(\hbar\omega)^2 - (2\Delta)^2}}. \quad (20)$$

Here p is the hole concentration, and

$$J = \int_0^\infty dy \exp\left(-y^2 - \frac{\Delta}{\Theta}\right) \cosh\left(\frac{\sqrt{\Delta^2 + \frac{\beta^2\Theta}{A}y^2}}{\Theta}\right). \quad (21)$$

C. Intrasubband transitions via the excited subband

At photon energy smaller than but comparable to the gap between the valence subbands, $\hbar\omega \leqslant 2\Delta$, optical absorption is caused by two-step transitions with an intermediate state in the excited subband (see Fig. 4). The shift current density in this case is given by [46]

$$\boldsymbol{j}^{\mathrm{intra}} = -2e\sum_{\boldsymbol{k},\boldsymbol{k}'} \frac{2\pi}{\hbar}\delta[E_1(\boldsymbol{k}) - E_1(\boldsymbol{k}') - \hbar\omega] \times \{f_0[E_1(\boldsymbol{k})] - f_0[E_1(\boldsymbol{k}')]\} \times \frac{\mathrm{Im}[W^*(\nabla_{\boldsymbol{k}} + \nabla_{\boldsymbol{k}'})W]}{[E_1(\boldsymbol{k}) + \hbar\omega - E_2(\boldsymbol{k} + \boldsymbol{q})]^2}, \quad (22)$$

with W being a product:

$$W = U^{12}_{\boldsymbol{k}',\boldsymbol{k}+\boldsymbol{q}} V_{21}. \quad (23)$$

Here V_{21} is a matrix element of direct optical transitions (18) introduced in the previous section, and $U^{12}_{\boldsymbol{k}',\boldsymbol{k}+\boldsymbol{q}}$ is the matrix element of intersubband scattering from state $(2,\boldsymbol{k}+\boldsymbol{q})$ to state $(1,\boldsymbol{k}')$, shown by the dashed line in Fig. 4. We assume the scattering to be elastic. Here we account only for the resonant term in the two-step transition matrix element which exceeds the other nonresonant one, at $\hbar\omega \approx 2\Delta$.

Since the wave-function envelopes are independent of $\boldsymbol{k}_\perp$, the scattering amplitude $U^{12}_{\boldsymbol{k}',\boldsymbol{k}+\boldsymbol{q}}$ can depend on only the difference $\boldsymbol{k}'_\perp - \boldsymbol{k}_\perp$. Hence, calculating the y photocurrent component, we should differentiate in W only the optical matrix element V_{21}. It is given by Eq. (18); therefore the elementary shifts coincide with those at direct intersubband transitions. Introducing the scattering time $\tilde{\tau}$ according to

$$\frac{1}{\tilde{\tau}} = \sum_{\boldsymbol{k}'} \frac{2\pi}{\hbar}\left|U^{12}_{\boldsymbol{k}',\boldsymbol{k}}\right|^2 \delta[E_1(\boldsymbol{k}) - E_1(\boldsymbol{k}') - \hbar\omega] \quad (24)$$

and neglecting a dependence of $\tilde{\tau}$ on $\boldsymbol{k}$ and ω, we obtain the photocurrent in the form

$$j_y^{\mathrm{circ,intra}} = -q_x i(E_x E_y^* - E_y E_x^*) \frac{p\, e^3 B|\beta|\sqrt{A}\varepsilon_\perp}{4J\Delta^2(\hbar\omega)^2\tilde{\tau}\sqrt{\Theta}\varepsilon_\parallel} \times (1 - e^{-\hbar\omega/\Theta}) \times \int_0^\infty dx \frac{\exp\left[-\frac{A\Delta^2}{\beta^2\Theta}x^2 + \frac{\Delta}{\Theta}(\sqrt{1+x^2} - 1)\right]}{(\sqrt{1+x^2} - \hbar\omega/2\Delta)^2(1+x^2)^{3/2}}. \quad (25)$$

Here J is introduced in Eq. (21).

The calculated CPDE current dependence on the light polarization at Drude-like, inter- and intrasubband optical transitions, Eqs. (15), (20), and (25), is in agreement with the phenomenological theory, Eqs. (3) and (6).

V. DISCUSSION

The developed theory of CPDE allows us to describe all experimental findings. In particular, both phenomenological and microscopic theories yield the experimentally observed dependence on the incidence angle [see Eq. (10) and the fit in Fig. 3]. However, although Fig. 2(b) demonstrates that the circular photocurrent is mainly an odd function of θ_0, an admixture of a small even contribution is present. In ideal tellurium, an even in θ_0 transverse photocurrent is forbidden by symmetry, and its presence in the studied sample is caused by some asymmetry in the xy plane. Indeed, the cross section of the grown single crystal does not represent a regular hexagon. The adjacent sides of the hexagonal cross section had different lengths, namely, 5 and 3 mm (see Fig. 1). This asymmetry appears in the process of growth: at the stretching of samples, an inhomogeneous distribution of the diameter is introduced due to pulsations of a heater. The nonideal samples have point symmetry group C_1. In this case, the even in θ_0 helicity-dependent currents are allowed due to both CPDE and the circular photogalvanic effect. A polarization-independent contribution to the transverse photocurrent [the term L_2 in Eq. (4)] is also caused by the above-mentioned asymmetry. Nevertheless, the dominating odd in θ_0 contribution is well described by the developed theory, which confirms observation of the CPDE.

Due to birefringence of tellurium (see Sec. III), the light circularly polarized in vacuum became elliptically polarized inside the sample. The presence of linear polarization can lead to additional photogalvanic currents caused by both the linear photon drag and the linear photogalvanic effects. The corresponding odd in θ_0 contribution behaves as $\propto P^0_{\mathrm{circ}}\theta_0^3$ at

small incidence angles. Our estimate shows that it does not exceed 20% of the CPDE contribution [Eq. (3)].

The CPDE current is an even function of the constant β (see Sec. IV). This result contrasts with the photocurrent caused by the circular photogalvanic effect, which is linear in β. The reason is that CPDE is insensitive to the presence of a space inversion center and therefore is the same in levorotatory tellurium and dextrorotatory tellurium, which are different by the sign of constant β.

Microscopic theory also describes the measured photon energy dependence presented in the inset in Fig. 3. The frequency dependencies of the transverse CPDE photocurrent for all three types of transitions considered above are shown in Fig. 4. At $\hbar\omega \ll \Theta < 2\Delta$, the frequency dependence is given by Eq. (15). This equation demonstrates that CPDE is present due to the energy dependence of the momentum relaxation time. Besides, it is also necessary to account for a uniaxiality of tellurium because CPDE is forbidden in systems with cubic symmetry. It follows from Eq. (15) that CPDE in tellurium exists due to anisotropy of the energy spectrum and the dielectric tensor. At $\omega\tau \ll 1$, the CPDE current increases linearly with frequency, $j_y^{\mathrm{circ,Drude}} \propto \omega$. At $\omega\tau \gg 1$ but still $\hbar\omega \ll \Theta$, the current decreases as $j_y^{\mathrm{circ,Drude}} \propto \omega^{-3}$. Both these asymptotes coincide with the high-frequency behavior of the CPDE current in graphene [8].

Near the direct absorption edge, $\hbar\omega = 2\Delta$, the CPDE current has a singularity corresponding to the transitions from the states with $k_z = 0$. It follows from Eq. (20) that above the direct absorption edge, $\hbar\omega \to 2\Delta + 0$, the coefficient T in the phenomenological equation (6) has a square-root singularity:

$$T_{\mathrm{inter}} = -\frac{pe^3 B|\beta|\sqrt{A}\pi\varepsilon_\perp}{4J\hbar\Delta^{5/2}\sqrt{\Theta}\varepsilon_\parallel}\frac{1-e^{-2\Delta/\Theta}}{\sqrt{\hbar\omega-2\Delta}}. \tag{26}$$

This singularity is a one-dimensional optical density of states which arises at direct optical transitions between the valence subbands. This van Hove singularity is not integrated because of equal energy dependencies on the perpendicular wave vector $k_\perp$ in both valence subbands.

Below the direct absorption edge, the singularity at $\hbar\omega \to 2\Delta - 0$ follows from the contribution to the integral equation (25) from $x = 0$, which yields

$$T_{\mathrm{intra}} = -\frac{\pi p\, e^3 B|\beta|\sqrt{A}\varepsilon_\perp}{16J\Delta^{5/2}\tilde{\tau}\sqrt{\Theta}\varepsilon_\parallel}\frac{1-e^{-2\Delta/\Theta}}{(2\Delta-\hbar\omega)^{3/2}}. \tag{27}$$

We see that the singularity is stronger at intraband transitions than at interband transitions by a factor $\sim\hbar/(|2\Delta - \hbar\omega|\tilde{\tau}) \gg 1$.

Experimental data demonstrate a decrease in the CPDE current $|J_{\mathrm{odd}}|$ with photon energy (see the inset in Fig. 3). Theoretically, we obtain a decrease in the current with frequency at direct intersubband transitions (for $\hbar\omega > 2\Delta$), as illustrated in Fig. 4. This explains qualitatively the spectral behavior of the CPDE current observed in experiment. The energy gap 2Δ in tellurium is about 126 meV [47], which is slightly larger than the two lowest photon energies used in the experiment. However, the photocurrent can be caused by direct optical transitions at all wavelengths because the energy gap may be reduced by deformations of the studied sample. We have estimated the CPDE current at intersubband transitions with the help of Eqs. (10) and (26). For tellurium at room temperature with $A = 3.71 \times 10^{-15}$ eV cm^2, $B = 3.57 \times 10^{-15}$ eV cm^2, $\beta = 2.5 \times 10^{-8}$ eV cm, and $2\Delta = 126$ meV [47], we obtain $\bar{j}/I \approx 50$ nA/W at $\hbar\omega = 130$ meV and $\theta_0 = 10^\circ$ (I is the light intensity). This is the same order of magnitude as that of the experimental data (see Fig. 3). Slightly smaller values of the current ($\sim$10 nA/W) are detected in the experiment because not all current generated in the laser spot area reaches the contacts. Part of the current is closed in the nonilluminated part of the sample.

VI. CONCLUSION

In conclusion, the helicity-dependent photocurrent transverse to the light incidence plane was detected in bulk tellurium. The above analysis of the polarization state, incidence angle, and photon energy dependencies of the photocurrent confirms the observation of the CPDE. The CPDE current is shown to be an odd function of the incidence angle. The phenomenological model of CPDE was developed based on symmetry arguments accounting for birefringence of tellurium. Microscopic theory for both inter- and intrasubband optical transitions was elaborated. The CPDE current was estimated by calculation of the shift contribution. The resonance in the CPDE current frequency dependence at the threshold of the intersubband transitions was demonstrated theoretically. Theory yielded the same photon energy dependence and values of the circular photocurrent as in the experiment. Due to the high sensitivity of CPDE, tellurium can be used for helicity-dependent photodetectors. This opens the way for all-electric detection of a light polarization state. Finally, we note that the CPDE current can be excited together with spin currents in topological insulators based on tellurides, and its study can be helpful for understanding their symmetry and kinetic properties.

ACKNOWLEDGMENTS

We thank S. D. Ganichev and E. L. Ivchenko for helpful discussions, I. V. Sedova for assistance in sample preparation, N. V. Ageev for help in transport measurements, and V. K. Kalevich for interest in the work. Financial support from the Russian Foundation for Basic Research, Ministry of Education and Science of the Russian Federation, and DFG (SPP 1666) is gratefully acknowledged. The work of L.E.G. was supported by the Russian Science Foundation (Project No. 14-12-01067).

APPENDIX : TRANSMISSION COEFFICIENT TO A UNIAXIAL MEDIUM

The amplitude of the ordinary beam $\boldsymbol{E} \parallel y$ at the boundary with vacuum ($z = 0$) is given by the Fresnel transmission coefficient for s-polarized light:

$$E_y(z=0) = \frac{2\cos\theta_0}{\cos\theta_0 + n_o}E_{0y}. \tag{A1}$$

Here $\boldsymbol{E}_0$ is the radiation amplitude in vacuum.

Under incidence of p-polarized light, the extraordinary beam is excited. From the Maxwell boundary conditions we obtain the amplitude of the transmitted wave at $z = 0$. For its

x component we have

$$E_x(z=0) = \frac{2n_e}{n_e + \varepsilon_\perp \cos\theta_0} E_{0x}. \quad \text{(A2)}$$

As a result, we have for bilinear combinations

$$E_x E_y = \frac{4n_e \cos\theta_0}{(\cos\theta_0 + n_o)(\varepsilon_\perp \cos\theta_0 + n_e)} E_{0x} E_{0y}. \quad \text{(A3)}$$

Since the circular polarization degree in vacuum $P^0_{\rm circ}$ is defined via

$$i\left(E_{0x}E^*_{0y} - E^0_{0y}E^*_{0x}\right) = P^0_{\rm circ} E_0^2 \cos\theta_0, \quad \text{(A4)}$$

the same combination for the transmitted light at the boundary with vacuum has the form

$$i(E_x E_y^* - E_y E_x^*)|_{z=0} = \mathcal{T}_{ps} P^0_{\rm circ} E_0^2, \quad \text{(A5)}$$

with $\mathcal{T}_{ps}$ given by Eq. (9).

[1] *Spin Physics in Semiconductors*, edited by M. I. Dyakonov (Berlin, Springer, 2008).
[2] *Handbook of Spin Transport and Magnetism*, edited by E. Y. Tsymbal and I. Zutic (CRC Press, Boca Raton, FL, 2011).
[3] Optical Orientation, edited by Y. Kusrayev and G. Landwehr, Semicond. Sci. Technol. **23**, 110301 (2008).
[4] A. Kirilyuk, A. V. Kimel, and T. Rasing, Rev. Mod. Phys. **82**, 2731 (2010).
[5] S. D. Ganichev and W. Prettl, J. Phys. Condens. Matter **15**, R935 (2003).
[6] E. L. Ivchenko and S. D. Ganichev, in *Spin Physics in Semiconductors*, edited by M. I. Dyakonov (Springer, Berlin, 2008), p. 245.
[7] *Spin Current*, edited by S. Maekawa, S. O. Valenzuela, E. Saitoh, and T. Kimura (Oxford University Press, Oxford, 2012).
[8] M. M. Glazov and S. D. Ganichev, Phys. Rep. **535**, 101 (2014).
[9] G. Usaj, P. M. Perez-Piskunow, L. E. F. Foa Torres, and C. A. Balseiro, Phys. Rev. B **90**, 115423 (2014).
[10] D. Yudin, O. Eriksson, and M. I. Katsnelson, Phys. Rev. B **91**, 075419 (2015).
[11] P. N. Lebedev, Ann. Phys. (Leipzig) **311**, 433 (1901).
[12] E. L. Ivchenko, *Optical Spectroscopy of Semiconductor Nanostructures* (Alpha Science, Harrow, UK, 2005).
[13] S. D. Ganichev and W. Prettl, *Intense Terahertz Excitation of Semiconductors* (Oxford University Press, Oxford, 2006).
[14] R. Loudon, S. M. Barnett, and C. Baxter, Phys. Rev. A **71**, 063802 (2005).
[15] A. Rogalski, *Infrared Detectors* (CRC Press, Boca Raton, FL, 2011).
[16] S. N. Danilov, B. Wittmann, P. Olbrich, W. Eder, W. Prettl, L. E. Golub, E. V. Beregulin, Z. D. Kvon, N. N. Mikhailov, S. A. Dvoretsky, V. A. Shalygin, N. Q. Vinh, A. F. G. van der Meer, B. Murdin, and S. D. Ganichev, J. Appl. Phys. **105**, 013106 (2009).
[17] E. Bründermann, H.-W. Hübers, and M. F. Kimmitt, *Terahertz Techniques*, Springer Series in Optical Sciences (Springer, Berlin, 2012).
[18] J. Maysonnave, S. Huppert, F. Wang, S. Maero, C. Berger, W. de Heer, T. B. Norris, L. A. De Vaulchier, S. Dhillon, J. Tignon, R. Ferreira, and J Mangeney, Nano Lett. **14**, 5797 (2014).
[19] P. A. Obraztsov, T. Kaplas, S. V. Garnov, M. Kuwata-Gonokami, A. N. Obraztsov, and Yu. P. Svirko, Sci. Rep. **4**, 4007 (2014).
[20] P. A. Obraztsov, N. Kanda, K. Konishi, M. Kuwata-Gonokami, S. V. Garnov, A. N. Obraztsov, and Yu. P. Svirko, Phys. Rev. B **90**, 241416 (2014).
[21] G. M. Mikheev, A. G. Nasibulin, R. G. Zonov, A. Kaskela, and E. I. Kauppinen, Nano Lett. **12**, 77 (2012).
[22] H. Kurosawa and T. Ishihara, Opt. Express **20**, 1561 (2012).
[23] E. L. Ivchenko and G. E. Pikus, in *Problems in Modern Physics*, edited by V. M. Tuchkevich and V. Ya. Frenkel (Nauka, Leningrad, 1980), p. 275 [in *Semiconductor Physics* (Consultant Bureau, New York, 1986), p. 427].
[24] V. I. Belinicher, Sov. Phys. Solid State **23**, 2012 (1981).
[25] O. Keller and G. Wang, Phys. Rev. B **56**, 12327 (1997).
[26] V. A. Shalygin, H. Diehl, Ch. Hoffmann, S. N. Danilov, T. Herrle, S. A. Tarasenko, D. Schuh, Ch. Gerl, W. Wegscheider, W. Prettl, and S. D. Ganichev, JETP Lett. **84**, 570 (2007).
[27] H. Diehl, V. A. Shalygin, V. V. Bel'kov, Ch. Hoffmann, S. N. Danilov, T. Herrle, S. A. Tarasenko, D. Schuh, Ch. Gerl, W. Wegscheider, W. Prettl, and S. D. Ganichev, New J. Phys. **9**, 349 (2007).
[28] T. Hatano, T. Ishihara, S. G. Tikhodeev, and N. A. Gippius, Phys. Rev. Lett. **103**, 103906 (2009).
[29] J. Karch, P. Olbrich, M. Schmalzbauer, C. Zoth, C. Brinsteiner, M. Fehrenbacher, U. Wurstbauer, M. M. Glazov, S. A. Tarasenko, E. L. Ivchenko, D. Weiss, J. Eroms, R. Yakimova, S. Lara-Avila, S. Kubatkin, and S. D. Ganichev, Phys. Rev. Lett. **105**, 227402 (2010).
[30] Ch. Jiang, V. A. Shalygin, V. Yu. Panevin, S. N. Danilov, M. M. Glazov, R. Yakimova, S. Lara-Avila, S. Kubatkin, and S. D. Ganichev, Phys. Rev. B **84**, 125429 (2011).
[31] P. Olbrich, C. Drexler, L. E. Golub, S. N. Danilov, V. A. Shalygin, R. Yakimova, S. Lara-Avila, S. Kubatkin, B. Redlich, R. Huber, and S. D. Ganichev, Phys. Rev. B **88**, 245425 (2013).
[32] L. Kang, S. Lan, Y. Cui, S. P. Rodrigues, Y. Liu, D. H. Werner, and W. Cai, Adv. Mater. **27**, 4377 (2015).
[33] S. Stachel, G. V. Budkin, U. Hagner, V. V. Bel'kov, M. M. Glazov, S. A. Tarasenko, S. K. Clowes, T. Ashley, A. M. Gilbertson, and S. D. Ganichev, Phys. Rev. B **89**, 115435 (2014).
[34] J. W. McIver, D. Hsieh, H. Steinberg, P. Jarillo-Herrero, and N. Gedik, Nat. Nanotechnol. **7**, 96 (2012).
[35] P. Olbrich, L. E. Golub, T. Herrmann, S. N. Danilov, H. Plank, V. V. Belkov, G. Mussler, Ch. Weyrich, C. M. Schneider, J. Kampmeier, D. Grützmacher, L. Plucinski, M. Eschbach, and S. D. Ganichev, Phys. Rev. Lett. **113**, 096601 (2014).
[36] V. A. Shalygin, A. N. Sofronov, L. E. Vorob'ev, and I. I. Farbshtein, Phys. Solid State **54**, 2362 (2012).
[37] S. D. Ganichev, U. Rössler, W. Prettl, E. L. Ivchenko, V. V. Bel'kov, R. Neumann, K. Brunner, and G. Abstreiter, Phys. Rev. B **66**, 075328 (2002).
[38] S. D. Ganichev, V. V. Bel'kov, Petra Schneider, E. L. Ivchenko, S. A. Tarasenko, W. Wegscheider, D. Weiss, D. Schuh,

E. V. Beregulin, and W. Prettl, Phys. Rev. B **68**, 035319 (2003).

[39] S. D. Ganichev, Ya. V. Terent'ev, and I. D. Yaroshetskii, Sov. Tech. Phys. Lett. **11**, 20 (1985).

[40] S. D. Ganichev, P. Schneider, V. V. Bel'kov, E. L. Ivchenko, S. A. Tarasenko, W. Wegscheider, D. Weiss, D. Schuh, B. N. Murdin, P. J. Phillips, C. R. Pidgeon, D. G. Clarke, M. Merrick, P. Murzyn, E. V. Beregulin, and W. Prettl, Phys. Rev. B **68**, 081302 (2003).

[41] S. D. Ganichev, Phys. B (Amsterdam, Neth.) **273**, 737 (1999).

[42] E. Ziemann, S. D. Ganichev, I. N. Yassievich, V. I. Perel, and W. Prettl, J. Appl. Phys. **87**, 3843 (2000).

[43] V. I. Belinicher, Phys. Lett. A **66**, 213 (1978).

[44] N. S. Averkiev, V. M. Asnin, A. A. Bakun, A. M. Danishevskii, E. L. Ivchenko, G. E. Pikus, and A. A. Rogachev, Sov. Phys. Semicond. **18**, 397 (1984).

[45] Note that accounting for an additional term in the elementary shift related to the Berry connection [12,48], is not necessary because it does not contribute to the photocurrent in the steady state [12].

[46] L. E. Golub and E. L. Ivchenko, J. Exp. Theor. Phys. **112**, 152 (2011).

[47] N. S. Averkiev, V. M. Asnin, A. A. Bakun, A. M. Danishevskii, E. L. Ivchenko, G. E. Pikus, and A. A. Rogachev, Sov. Phys. Semicond. **18**, 402 (1984).

[48] J. E. Sipe and A. I. Shkrebtii, Phys. Rev. B **61**, 5337 (2000).